

RESEARCH ARTICLE | AUGUST 30 2017

## Highly stretchable electrospun conducting polymer nanofibers

SCI F 

Fanny Boubée de Gramont; Shiming Zhang; Gaia Tomasello; Prajwal Kumar; Andranik Sarkissian ; Fabio Cicoira 

 Check for updates

*Appl. Phys. Lett.* 111, 093701 (2017)

<https://doi.org/10.1063/1.4997911>

 View  
Online

 Export  
Citation

# Highly stretchable electrospun conducting polymer nanofibers

Fanny Boubée de Gramont,<sup>1</sup> Shiming Zhang,<sup>1</sup> Gaia Tomasello,<sup>1</sup> Prajwal Kumar,<sup>1</sup> Andranik Sarkissian,<sup>2</sup> and Fabio Cicoira<sup>1,a)</sup>

<sup>1</sup>Department of Chemical Engineering, Polytechnique Montreal, Montreal, Quebec H3C 3A7, Canada

<sup>2</sup>Plasmionique, Inc., 171-1650 boul. Lionel Boulet, Varennes, Quebec J3X 1S2, Canada

(Received 13 March 2017; accepted 26 July 2017; published online 30 August 2017)

Biomedical electronics research targets both wearable and biocompatible electronic devices easily adaptable to specific functions. To achieve such goals, stretchable organic electronic materials are some of the most intriguing candidates. Herein, we develop highly stretchable poly-(3,4-ethylenedioxythiophene) (PEDOT) doped with tosylate (PEDOT:Tos) nanofibers. A two-step process involving electrospinning of a carrier polymer (with oxidant) and vapor phase polymerization was used to produce fibers on a polydimethylsiloxane substrate. The fibers can be stretched up to 140% of the initial length maintaining high conductivity. *Published by AIP Publishing.*

[<http://dx.doi.org/10.1063/1.4997911>]

Organic electronic materials present intriguing properties that are specifically interesting for biological applications: they can interface with aqueous solutions without leading to the formation of an oxide layer, thus favoring direct contact with the biological milieu, and can support a mixed ionic/electronic conduction.<sup>1,2</sup> These properties, together with ease of process and possibility of tuning properties via chemical synthesis, make organic electronic devices good candidates for biomedical applications such as sensing and stimulation/recording of brain activity.<sup>3,4</sup> Other desirable characteristics for applications in bioelectronics are flexibility and stretchability, which permit us to accommodate devices on objects with irregular shapes.<sup>2</sup> Two main strategies are used to achieve stretchable organic electronics, i.e., using intrinsically stretchable materials, or impart stretchability using substrates with buckled geometry.<sup>5-7</sup> Alternatively, structures such as fibers can be used to improve the stretchability of poorly stretchable materials such organic conducting polymers.<sup>8,9</sup> To date, several techniques have been used to obtain conductive fibers, such as drawing,<sup>10</sup> template synthesis,<sup>11</sup> phase separation,<sup>12</sup> wet-spinning,<sup>8,13,14</sup> and electrospinning.<sup>9,15</sup> Drawing consists of mechanically pulling a liquid to stretch it into thin filaments and let it solidify. As such, it can only be used for fluids with a high viscoelasticity which are resistant enough to be drawn without breaking under the stress caused by the process. Template synthesis permits us to obtain fibers by synthesizing the desired materials within the pores of a membrane with an adequate diameter. Phase separation is a complex process that yields nanoporous polymer membranes that can be used directly as a fibrous scaffold. It necessitates polymer dissolution, phase separation and gelation, solvent extraction, freezing, and freeze-drying under vacuum, making it both a long and complex process. Wet-spinning consists of pushing a liquid through a nozzle towards a coagulation bath to obtain solidification of the filaments. This process yields fibers with large diameters (typically more than 10  $\mu\text{m}$ ),

which limits their potential applications. Electrospinning is a more viable technique to produce nanofibers of various kinds of polymers with average diameters ranging from a few tens of nm to a few tens  $\mu\text{m}$ , depending on the parameters chosen for the process.<sup>16,17</sup> It uses an electrostatic force to spin polymer fibers from the tip of a syringe needle (or spinneret) containing a polymer solution. The spinneret is maintained at a high voltage (typically tens of kV) with respect to a grounded target substrate (collector). When the electrostatic force overcomes the surface tension of the polymer solution, the liquid spills out of the spinneret and forms thin filaments, which are collected on the substrate. Electrospinning permits tuning of the diameters of the fibers and their morphology, simply by changing parameters, such as voltage applied between the needle and the collector, distance between the needle and the collector, injection speed, duration of the spinning, type of collector used, and viscosity of the polymer solution.<sup>18,19</sup> Despite the advantages of electrospinning, conjugated polymers are difficult to process with this technique because their rigid backbone does not allow them to reach the level of chain entanglement required for the formation of fibers.<sup>17</sup> Therefore, electrospinning of conjugated polymers is typically achieved in combination with other techniques such as vapor phase polymerization (VPP),<sup>20,21</sup> oxidative polymerization,<sup>22</sup> and wet spinning,<sup>23</sup> or by adding high-viscosity materials to a conducting polymer suspension.<sup>24,25</sup> In this letter, we obtained poly(3,4-ethylenedioxythiophene) PEDOT doped with Tosylate (PEDOT:Tos) fibers on polydimethylsiloxane (PDMS), by first electrospinning fibers containing an oxidant with a carrier polymer, followed by vapor phase polymerization. The fibers show high stretchability while remaining conductive up to ca. 140% strain. This work paves the way for developing highly stretchable organic electronics for applications in conformable biomedical devices and stretchable interconnects for wearable electronics.

PDMS substrates (thickness of about 300  $\mu\text{m}$ ) were prepared by spin coating a 10:1 mixture of the elastomer and its curing agent (Sylgard<sup>®</sup> 184 Silicone Elastomer kit, Dow Corning) at 500 revolutions per minute (rpm) for 30 s on a glass substrate treated with a 10<sup>-3</sup> M solution (500 rpm for

<sup>a)</sup>Author to whom correspondence should be addressed: Fabio.cicoira@polymtl.ca

30 s) of hexadecyltrimethylammonium bromide (CTAB, Sigma-Aldrich). The CTAB treatment is necessary to facilitate successive peel-off of PDMS from glass. The PDMS was then baked at 90 °C for 30 min before being gently peeled off from the slide. It was then attached to the cylindrical metallic collector of an RT-collector electrospinning setup (Linari Engineering) equipped with a cylindrical collector. Electrospinning of fibers of the carrier polymer polyvinylpyrrolidone (PVP, step 1 in Fig. 1) was carried out with a mixture obtained adding 0.23 g of PVP at  $M_w \approx 1\,300\,000$  (Sigma-Aldrich) and 0.73 g of the weak base imidazole (Sigma-Aldrich) to 22.6 g of a solution of the oxidant Fe(III)Tos in butanol (CLEVIOS C-B 54 V3, Heraeus Electronic Materials GmbH), which acts as a polymerization initiator. The mixture was homogenized before use with a planetary mixer. This composition is based on a previously reported procedure that we optimized for electrospinning on PDMS.<sup>20</sup> Imidazole acted as a weak base during the polymerization step to prevent the reaction milieu from becoming acidic, which would lead to a side reaction producing non-conductive species.<sup>26</sup> The mixture was diluted 4:1 into isopropyl alcohol, thoroughly mixed, and transferred into a 5 ml glass syringe with a needle having a diameter of 0.8 mm. The syringe was placed on a syringe pump (Razel Scientific) to ensure a constant flow of the mixture during electrospinning. We performed electrospinning for 3 min with a flow of 2 ml/h, with the collector rotating at 500 rpm, keeping a distance of 15 cm between the tip of the needle and the metallic

collector and applying a 20 kV voltage between the needle and the grounded collector. These parameters allowed for a satisfactory density of the final fiber mat, without risking delamination from PDMS. The process resulted in a non-woven mat of nanofibers made of PVP imidazole and Fe(III)Tos. According to the literature, the oxidant and the proton acceptor are found in higher concentrations in the external layer of the fibers.<sup>18</sup> After electrospinning, the fibers were transferred to a Vapor Phase Polymerization (VPP) reactor, where they were exposed to vapors of the monomer 3,4-ethylenedioxothiophene (EDOT, Sigma Aldrich, step 2 in Fig. 1). When in contact with the fibers containing the oxidant, EDOT polymerized to yield PEDOT doped with the counter ion tosylate, i.e., PEDOT:Tos. We set the exposure time of the fibers to EDOT to 30 min. Based on electrical conductivity measurements and visual inspection, we estimate this time to be long enough for the polymerization to occur, while avoiding the full consumption of imidazole, which would lead to the formation of insulating species. After polymerization, the samples were rinsed with ethanol (Sigma-Aldrich) using a “double-puddle” method (step 3 in Fig. 1): they were fixed on the chuck of a spin-coater, covered with ethanol for 30 s, and then spun at 500 rpm for 30 s to remove the ethanol. This procedure was performed twice for each sample. This method was chosen to prevent any delamination of the fiber film from PDMS, which may occur upon a complete immersion in ethanol. The main purpose of this last step is to remove unreacted species (monomer and imidazole), oxidant residues, and nonconductive species generated by side reactions. As PVP is soluble in ethanol, this step also dissolves the core of the fibers, leading to a material which is more stable in ambient air. Indeed, PVP can easily react with the ambient humidity and melt by absorbing water, which could compromise the properties of the fiber mat over the long term. A relatively high current (of the order of tens of mA) could be recorded by placing electrodes at the two extremities of our samples, although the electrical conductivity could not be extracted due to the difficulty to measure the thickness of the fiber mat.

Images of the fibers were taken by using a JEOL FEG-SEM, JSM 7600F scanning electron microscope (FE-SEM) and by optical microscopy using a Zeiss Imager M1 microscope equipped with an AxioCam MRm camera by Carl Zeiss. The combination of electrospinning, VPP, and ethanol rinsing resulted in randomly oriented fibers. SEM images show that after ethanol rinsing, most of the fibers appeared flatter, thinner, and with a smoother surface [Figs. 2(a) and 2(b)]. This confirms the removal of the PVP core, which leads to the partial collapse of the PEDOT:Tos fibers, as well as the removal of unreacted species from the surface of the fibers. Some of the fibers also presented small beaded structures [Fig. 2(a)], which could be explained by a partial melting of the PVP fibers before the start of the VPP step, due to the ambient humidity. The SEM images were used to estimate the average diameter of the fibers (using the ImageJ software from the National Institute of Health), which for rinsed fibers was of about 700 nm over an area of  $480 \times 360 \mu\text{m}^2$ .

Our PEDOT:Tos fibers on PDMS show excellent properties as stretchable conductors. Most of the fibers follow the

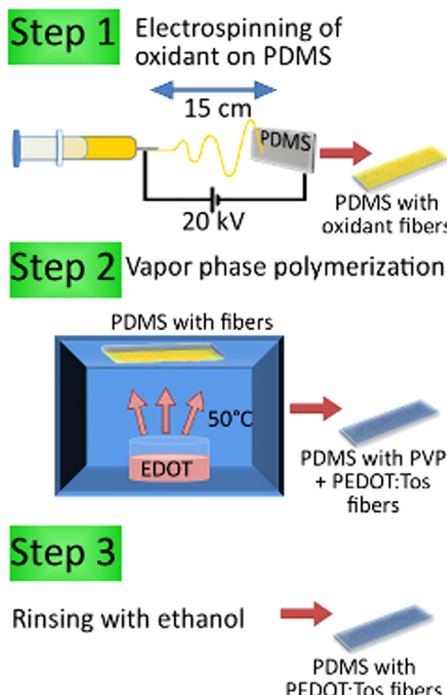


FIG. 1. Process used to obtain fibers of PEDOT:Tos. A mixture containing PVP, Fe(III)Tos, and Imidazole is electrospun on a PDMS substrate attached to a rotating cylindrical collector. The applied voltage is 20 kV, and the distance is 15 cm (step 1). The PDMS covered with fibers is placed inside a chamber at atmospheric pressure. A crucible containing EDOT is warmed at 50 °C to evaporate the monomer, thus allowing the polymerization of PEDOT:Tos on the fibers (step 2). The fibers are rinsed with ethanol to remove the unreacted chemicals (monomer and oxidant) and to dissolve the PVP core (step 3).

stretching of the PDMS substrate without breaking. By comparing intact fibers [Fig. 2(c)] with stretched ones [Fig. 2(d)], it is possible to notice a few broken fibers and small tears in the mat, perpendicular to the stretching direction. We hypothesize that the distortion of the fibers and the appearance of these small localized tears absorb the strains during stretching without the appearance of bigger cracks that would rupture the whole mat apart.

The electrical properties of our fibers under stretching were studied using a home-made computer-controlled tensile tester. Eutectic Gallium-Indium (EGaIn, Sigma-Aldrich) was used to form two liquid contacts [see the inset in Fig. 3(a)] to ensure a good connection between the PEDOT:Tos fibers and copper wires connected to an Agilent B2902A source measure unit. A constant voltage of 200 mV was applied during the measurement.

The ability of the PEDOT:Tos fibers to conduct the current under stretching was tested by monitoring the temporal evolution of the current during consecutive stretching cycles at strain percentages ranging from 20% to 140% with respect to the initial sample length. The applied strain percentage is defined as  $[(L' - L)/L] \times 100\%$ , where  $L$  and  $L'$  denote the relaxed and stretched lengths of the PDMS substrate, respectively (e.g., a strain percentage of 20% means a 3-cm film is elongated by 20% of its initial length, reaching 3.6 cm). Figure 3(a) shows the current vs time evolution for five cycles with resting times at different applied strains. The film was first stretched at 20%, kept in this state for one minute, and released to its initial length for 1 min. This process was repeated for five times. The same procedure was applied for applied strains of 40%, 60%, 80%, 100%, 120%, and 140%. The PDMS substrate broke when a 160% strain was applied. Surprisingly, the fibers stretched up to a 140% strain percentage still retained 15%–20% of the initial current (i.e., a final current of about  $2.5 \times 10^{-5}$  A vs an initial current of  $1.5 \times 10^{-4}$  A). Figure 3(a) shows that, each time an increasing strain is applied, the current decreases by a

certain amount (about 10%–15% of the initial current), due to the rupture of certain fibers in the mat. After this decrease, the current remains stable during the successive four stretching and releasing at the same strain percentage. Figure 3(b) shows the current vs time evolution for a sample stretched to 100% of its initial length for 50 cycles. For each cycle, a first 100% strain was performed, and then, the film was released immediately to its initial length. Each full cycle lasted a total of 30 s (15 s stretching, 15 s releasing), and this process was performed 50 times. After an initial increase during the first cycle, likely due to contacts between initially separated fibers, the current reaches a stable value (about 50% of the initial current) after about 30 cycles, which confirms the high stretchability of our PEDOT:Tos fibers on PDMS.

During any stretching or releasing event, the current inside the fibers show a small spike. This is probably due to dynamic rearrangements of the conductive pathways inside the non-woven fabric, as suggested by the relative regularity of the patterns in these spikes. These rearrangements are transitory; lower currents are thus obtained once the fibers are in a steady-state compared to the transitory state. These differences are, however, small, and the current after the first few stretches remains almost constant, with variations within 2% of the initial current between the stretched and the released states.

Remarkably, the complete loss of conductivity in these fibers is systematically due to the breaking of the PDMS substrate rather than breaking of the fibers themselves. It is expected that our fibers could be stretched much more than 140% if deposited on a more stretchable substrate rather than on PDMS. However, it is important to note that a stretchability of 140% is an excellent value for biomedical and wearable applications. By comparison, simple PEDOT:Tos films made by spin-coating a layer of the same mixture and using vapor phase polymerization cannot be stretched more than 10% of their initial length without fracturing, independently from the strength of the PDMS.

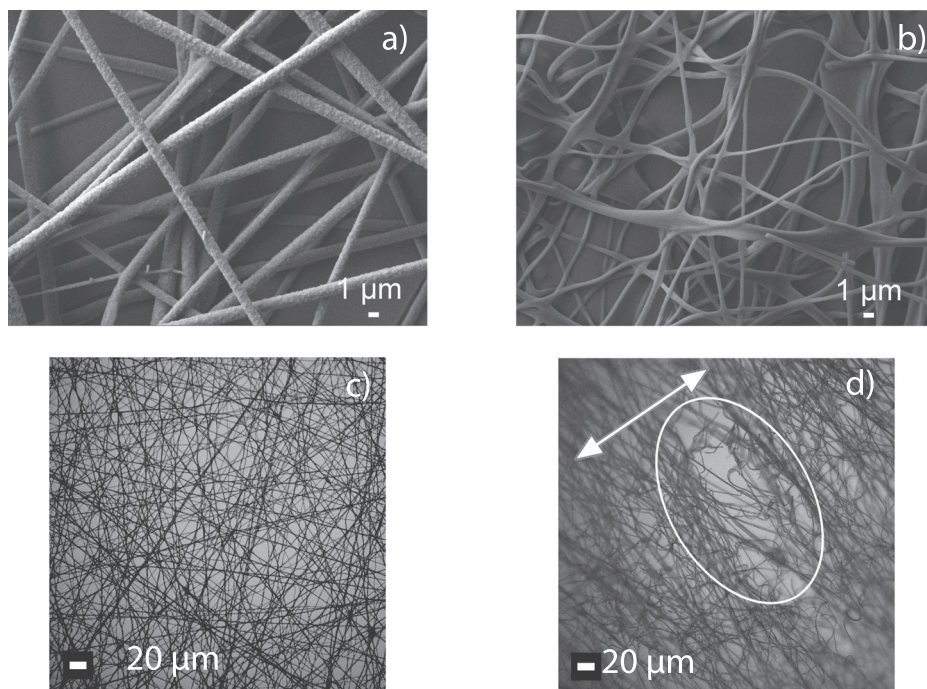


FIG. 2. (a) SEM micrograph of a network of fibers (a) before and (b) after rinsing in ethanol. The “flatness” of the fibers is due to the removal of the PVP core following rinsing with ethanol (the scale bar is 1  $\mu$ m). (c) and (d) Optical microscopy of a network of fibers (c) before and (d) after a 100% stretch. The white arrow shows the stretching direction, and the oval highlights a small tear in the network, as well as a few broken fibers [the scale bar in (c) and (d) is 20  $\mu$ m]. The fibers were electrospun for 3 min at 20 kV with a 15 cm nozzle-collector distance, followed by 30 min of VPP.

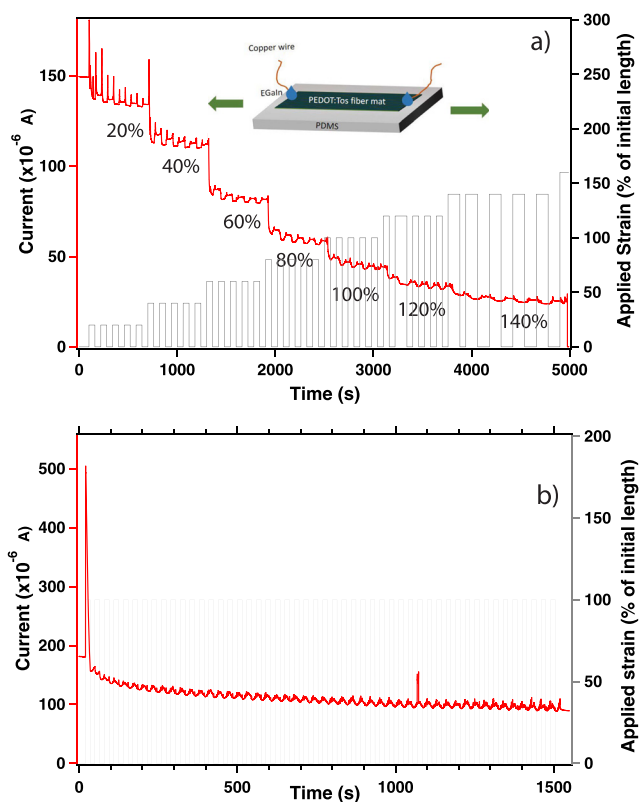


FIG. 3. (a) Current vs time plots for PEDOT:Tos fibers on PDMS. The sample was stretched from 20% to 140% strain percentages at 0.1 cm/s. Five consecutive cycles of stretching and release were performed at each of the different strain percentages between 20% and 140%. The PDMS substrate broke at 160% strain. The samples were kept in each state (stretched or released) for a resting time of 1 min. Inset: the scheme of the setup used for this measurement. EGaIn was used for the connection between the fiber mat and the copper wires. (b) Current vs time plots for a similar sample stretched at 100% strain percentage for 50 cycles, with a stretching speed of 0.1 cm/s. One stretching cycle consisted of stretching at 100% strain during 15 s followed by release to the initial length during 15 s. The 50 cycles were performed without pause. The samples were 1.5 cm long and 1 cm wide. The fibers were obtained after 3 min of electrospinning at 20 kV and 15 cm nozzle-collector distance, 30 min of VPP, and rinsing with ethanol. The measurements were made at 200 mV.

In conclusion, using a combination of electrospinning and vapor phase polymerization, we obtained stretchable conducting PEDOT:Tos fibers with an average diameter of about 700 nm directly on PDMS. These fibers were stretched, while a 200 mV bias was applied. After initial current loss at each new stretching percentage, the current appeared to be stable, and the films could be brought back to their initial length, while keeping a relatively high conductivity, up to applied strains as high as 140%. These results demonstrate that electrospinning of conducting polymer nanofibers on PDMS constitutes an alternative and complementary approach to other more established ones, such as buckling and mixing with elastomers, to achieve stretchable conductors. We believe that the performance of our stretchable nanofibers can be further improved by depositing the fibers on a pre-strained substrate, adding plasticizers or high-viscosity materials to the electrospinning solution, and controlling the fibers density, alignment, and diameter via the electrospinning voltage and the needle-collector distance. Another approach to improve the stretchability would be to make use of the secondary bending instability that appears in

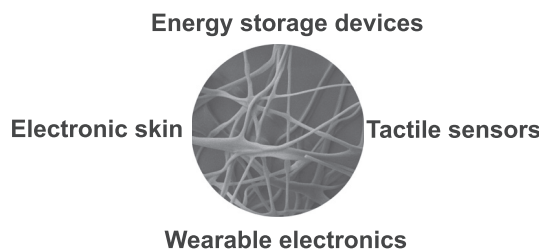


FIG. 4. Potential application of conducting polymer stretchable nanofibers.

electrospinning when the distance between the spinneret and the collector is increased. This is expected to lead to fiber mats that would tend to bend or coil on themselves. Due to this shape, it is expected that higher strains could be applied before observing a clear drop in conductivity.

Methods such as pre-stretching and buckling or adding plasticizer to the PEDOT fibers can be explored in the future to further increase the stretchability of our fibers. The current stability upon stretching makes these fibers an interesting candidate for biomedical applications *in vivo* and *in vitro* requiring conformable and stretchable electronics, such as implantable surface electrodes, electronic skin, touch sensors, and conductive cell culture scaffold. In addition, PEDOT:PSS nanofibers can be employed as a channel in electrochemical transistors, to be used as conformable devices for *in vivo* recording, stimulation, and drug delivery and for charge storage devices, such as supercapacitors (Fig. 4).

The authors are grateful to D. Pilon for technical support. This work was supported by the grants Discovery (NSERC), Engage 493111 2015 (NSERC), Établissement de Nouveau Chercheur (FRQNT), PSR-SIIRI 956 (Québec MESI), and John Evans Research Fund (CFI) awarded to F.C. S.Z. is grateful to NSERC for financial support through a Vanier Canada Graduate Scholarship. F.B.G. is grateful to GRSTB for financial support through a scholarship. We have also benefited from the support of CMC Microsystems through the program MNT financial assistance and FRQNT and its Regroupement stratégique program through a grant awarded to RQMP. GT acknowledges the Trottier Energy Institute for financial support.

- <sup>1</sup>J. Rivnay, R. M. Owens, and G. G. Malliaras, *Chem. Mater.* **26**, 679 (2014).
- <sup>2</sup>Z. Bao and X. Chen, *Adv. Mater.* **28**, 4177 (2016).
- <sup>3</sup>S. H. Kim, K. Hong, W. Xie, K. H. Lee, S. Zhang, T. P. Lodge, and C. D. Frisbie, *Adv. Mater.* **25**, 1822 (2013).
- <sup>4</sup>M. R. Abidian and D. C. Martin, *Biomaterials* **29**, 1273 (2008).
- <sup>5</sup>W. Zeng, L. Shu, Q. Li, S. Chen, F. Wang, and X. M. Tao, *Adv. Mater.* **26**, 5310 (2014).
- <sup>6</sup>S. Savagatrup, E. Chan, S. M. Renteria-Garcia, A. D. Printz, A. V. Zaretzki, T. F. O'Connor, D. Rodriguez, E. Valle, and D. J. Lipomi, *Adv. Funct. Mater.* **25**, 427 (2015).
- <sup>7</sup>S. Zhang, E. Hubis, G. Tomasello, G. Soliveri, P. Kumar, and F. Cicoira, *Chem. Mater.* **29**, 3126 (2017).
- <sup>8</sup>M. Z. Seyedin, J. M. Razal, P. C. Innis, and G. G. Wallace, *Adv. Funct. Mater.* **24**, 2957 (2014).
- <sup>9</sup>B. Sun, Y. Z. Long, Z. J. Chen, S. L. Liu, H. D. Zhang, J. C. Zhang, and W. P. Han, *J. Mater. Chem. C* **2**, 1209 (2014).
- <sup>10</sup>T. Ondarçuhu and C. Joachim, *Europhys. Lett.* **42**, 215 (1998).
- <sup>11</sup>C. R. Martin, *Chem. Mater.* **8**, 1739 (1996).
- <sup>12</sup>P. X. Ma and R. Zhang, *J. Biomed. Mater. Res.* **46**, 60 (1999).
- <sup>13</sup>S. J. Pomfret, P. N. Adams, N. P. Comfort, and A. P. Monkman, *Polymer* **41**, 2265 (2000).

<sup>14</sup>H. Okuzaki, Y. Harashina, and H. Yan, *Eur. Polym. J.* **45**, 256 (2009).

<sup>15</sup>J. Fang, H. Shao, H. Niu, and T. Lin, “Applications of electrospun nanofibers for electronic devices,” in *Handbook of Smart Textiles* (Springer, Berlin, Germany, 2015), pp. 617–652.

<sup>16</sup>S. Agarwal, A. Greiner, and J. H. Wendorff, *Prog. Polym. Sci.* **38**, 963 (2013).

<sup>17</sup>Y. Z. Long, M. M. Li, C. Gu, M. Wan, J. L. Duvail, Z. Liu, and Z. Fan, *Prog. Polym. Sci.* **36**, 1415 (2011).

<sup>18</sup>G. C. Rutledge and S. V. Fridrikh, *Adv. Drug Delivery Rev.* **59**, 1384 (2007).

<sup>19</sup>S. L. Shenoy, W. D. Bates, H. L. Frisch, and G. E. Wnek, *Polymer* **46**, 3372 (2005).

<sup>20</sup>A. Laforgue and L. Robitaille, *Macromolecules* **43**, 4194 (2010).

<sup>21</sup>O. S. Kwon, S. J. Park, J. S. Lee, E. Park, T. Kim, H. W. Park, S. A. You, H. Yoon, and J. Jang, *Nano Lett.* **12**, 2797 (2012).

<sup>22</sup>X. Li, T. Gu, and B. Wei, *Nano Lett.* **12**, 6366 (2012).

<sup>23</sup>D. Esrafilzadeh, R. Jalili, X. Liu, K. J. Gilmore, J. M. Razal, S. E. Moulton, and G. G. Wallace, *J. Mater. Chem. B* **4**, 1056 (2016).

<sup>24</sup>B. Bessaire, M. Mathieu, V. Salles, T. Yeghoyan, C. Celle, J.-P. Simonato, and A. Brioude, *ACS Appl. Mater. Interfaces* **9**, 950 (2017).

<sup>25</sup>J. Choi, J. Lee, J. Choia, D. Jungb, and S. E. Shima, *Synth. Met.* **160**, 1415 (2010).

<sup>26</sup>B. Winther-Jensen, D. W. Breiby, and K. West, *Synth. Met.* **152**, 1 (2005).